

Published in final edited form as:

J Am Chem Soc. 2011 May 11; 133(18): 7229–7233. doi:10.1021/ja202091a.

Entropic and enthalpic components of catalysis in the mutase and lyase activities of *Pseudomonas aeruginosa* PchB

Qianyi Luo, Kathleen M. Meneely, and Audrey L. Lamb*

Molecular Biosciences, University of Kansas, Lawrence, Kansas 66045

Abstract

The isochorismate-pyruvate lyase from *Pseudomonas aeruginosa* (PchB) catalyzes two pericyclic reactions, demonstrating the eponymous activity and also chorismate mutase activity. The thermodynamic parameters for these enzyme-catalyzed activities, as well as the uncatalyzed isochorismate decomposition, are reported from temperature dependence of k_{cat} and k_{uncat} data. The entropic effects do not contribute to enzyme catalysis as expected from previously reported chorismate mutase data. Indeed, an entropic penalty for the enzyme-catalyzed mutase reaction ($\Delta S^\ddagger = -12.1 \pm 0.6$ cal/molK) is comparable to that of the previously reported uncatalyzed reaction, whereas that of the enzyme-catalyzed lyase reaction ($\Delta S^\ddagger = -24.3 \pm 0.6$ cal/molK) is larger than that of the uncatalyzed lyase reaction (-15.77 ± 0.02 cal/molK) documented here. With the assumption that chemistry is rate-limiting, we propose that a reactive substrate conformation is formed upon loop closure of the active site and that ordering of the loop contributes to the entropic penalty for converting the enzyme substrate complex to the transition state.

The isochorismate-pyruvate lyase (PchB) from *Pseudomonas aeruginosa* catalyzes an asynchronous [1,5]-sigmatropic shift with a hydrogen transfer from C2 to C9 that has been shown to have a pericyclic transition state: the enzyme-catalyzed reaction shows quantitative transfer of the C2 hydrogen and a ^2H kinetic isotope effect consistent with the elimination reaction ¹ (Figure 1a). PchB also exhibits chorismate mutase (CM) activity (Figure 1b), which is a pericyclic reaction, albeit more than two orders of magnitude less efficient than physiological chorismate mutases ^{2,3}. Therefore, this enzyme performs two related pericyclic reactions in a single active site with a considerable difference in efficiency.

PchB is neither structurally nor functionally homologous to the pyruvate lyases of other shikimic acid metabolites ⁴⁻⁶. Instead, PchB shares homology with the chorismate mutases of the AroQ structural class, including *E. coli* chorismate mutase (EcCM) ⁷. EcCM is actually the N-terminal domain of a two-domain multifunctional prephenate dehydratase that was cloned separately and purified ⁸. The structure of EcCM reveals an intertwined dimer of three helices each with two equivalent buried active sites composed of residues from each subunit ⁹. A transition state analogue (TSA) is bound in the active site, oriented by arginine residues that align the carboxylates. In contrast, the chorismate mutase from *B. subtilis* (BsCM) is a member of the AroH structural class, and is a trimer which forms a pseudo- $\alpha\beta$ -barrel with three equivalent active sites at the subunit interfaces. The same TSA is bound in one of the solved structures, and is oriented in the active site by comparable arginines ^{10,11}. Apo- and prephenate-bound structures of BsCM have also been completed ^{10,12}. Despite the overall structural differences between the two classes, the active sites of EcCM and BsCM are usually considered comparable due to their shape and charge complementarity ¹³.

*corresponding author; phone: (785)864-5075; fax: (785)864-5294; lamb@ku.edu.

Less is known about the structures of the chorismate mutases from *Klebsiella pneumoniae* (KpCM; formerly *Aerobacter aerogenes*) and *Streptomyces aureofaciens* (SaCM), as the original work was completed on enzyme purified from bacterial culture¹⁴. A BLAST¹⁵ search reveals that *K. pneumoniae* has a prephenate dehydratase analogous to EcCM, and an alignment reveals that the CM domains share 92% sequence identity (all sequence comparisons were calculated using L-ALIGN¹⁶). Early work suggested two CM active sites¹⁴, so we will classify this enzyme as a member of the AroQ family. *S. aureofaciens*, in contrast, contains a monofunctional chorismate mutase that shares sequence homology to BsCM (38% identity, 64% similarity). SaCM was originally thought to have two or four subunits per oligomer¹⁴, but in recent work the calculations have assumed trimeric enzyme¹⁷. We will classify this enzyme as a member of the AroH family.

There has been the assertion that the enzyme-catalyzed chorismate mutase reaction is entropically driven^{14,18}, though this is a matter of debate¹⁷. This hypothesis is proposed from temperature dependence of k_{cat} data from both structural classes of chorismate mutases. We report herein the thermodynamic parameters, entropic and enthalpic contributions to the free energy of activation, for both the lyase and mutase reactions of PchB, and for the uncatalyzed lyase reaction, and compare these data to those reported previously for the AroQ and AroH chorismate mutases.

Materials and Methods

Protein preparation

Wild-type PchB without a histidine tag was prepared as previously described⁷.

Preparation of isochorismate and chorismate

Isochorismate was isolated from *K. pneumoniae* 62-1 harboring the *entC* plasmid pKS3-02¹⁹ with only minor changes, as described previously³. Chorismate (Sigma, 60-80% pure) was recrystallized as previously described²⁰.

Chorismate mutase (CM) activity assays

Initial velocities were measured in 50 mM sodium/potassium phosphate buffer pH 7.5 at temperatures from 5 °C to 45 °C by measuring chorismate disappearance at 310 nm with a Cary 50 Bio spectrophotometer (Varian) and an electrothermal single cell holder for temperature control (± 0.1 °C). Enzyme (80 μM) was incubated for 10 min at the desired temperature, and the reaction was initiated by the addition of chorismate, varied in concentration from 0.05 mM to 1.4 mM. Kinetic data were fit to the Michaelis-Menten equation by the nonlinear regression function of KaleidaGraph (Synergy Software).

Isochorismate-pyruvate lyase (IPL) activity assays

Initial velocities were measured in 50 mM sodium/potassium phosphate buffer pH 7.5 at temperatures from 5 °C to 45 °C by measuring the accumulation of salicylate by fluorescence with an excitation wavelength of 300 nm and an emission wavelength of 430 nm using a Cary Eclipse fluorescence spectrophotometer (Varian) and an electrothermal single cell holder for temperature control (± 0.1 °C). Enzyme (0.25 μM) was incubated for 10 min at the desired temperature, and the reaction was initiated by the addition of chorismate, varied in concentration from 2 μM to 32 μM . Kinetic data were fit to the Michaelis-Menten equation by the nonlinear regression function of KaleidaGraph (Synergy Software).

Calculation of Thermodynamic Activation Parameters

The activation enthalpy (ΔH^\ddagger) and entropy (ΔS^\ddagger) were determined from the linear regression of the data collected from 5 °C to 45 °C according to the Eyring equation ²¹:

$$k_{\text{cat}} = \left(\frac{kT}{h} \right) e^{-\left[\left(\frac{\Delta H^\ddagger}{RT} \right) - \left(\frac{\Delta S^\ddagger}{R} \right) \right]}$$

where **k** is Boltzmann's constant, **h** is Planck's constant, **R** is the ideal gas constant, and **T** is the temperature in Kelvin.

Uncatalyzed Decomposition of Isochorismate in Solution

Isochorismate undergoes elimination to form salicylate and pyruvate and rearrangement to form isoprephenate in the absence of enzyme ²². Salicylate formation was monitored in water at temperatures from 30 °C to 70 °C by monitoring fluorescence with an excitation wavelength of 310 nm and an emission wavelength of 430 nm using a Cary Eclipse fluorescence spectrophotometer (Varian) and an electrothermal single cell holder for temperature control (± 0.1 °C). The amount of salicylate formed was determined with a standard curve (0 – 50 μM). The rate of isochorismate disappearance (*k*) was determined from the plot of salicylate formation (*y*) versus time (*t*) according to the equation:

$$y = a(1 - e^{-kt})$$

where $a = I_0(k_1/k)$, $k = k_1 + k_2$, and $I_0 = 350 \mu\text{M}$ (the initial isochorismate concentration). k_1 is the rate for the elimination reaction and k_2 is the rate for the Claisen rearrangement. Thermodynamic activation parameters for the elimination and rearrangement reactions were calculated from the corresponding Eyring plots.

Results and Discussion

Model for the entropic contribution to the transition from the enzyme-substrate complex to the transition state

The experiments described here and those from previous work used for comparison all report the temperature dependence of k_{uncat} or k_{cat} . These data therefore reflect changes in free energy, enthalpy and entropy for converting the free substrate (*S*) to the free transition state (S^\ddagger) in the case of k_{uncat} or the enzyme substrate complex (*ES*) to the transition state (ES^\ddagger) in the case of k_{cat} . The entropic component for formation of the ES^\ddagger for the reactions discussed range from an equal or larger penalty than that observed for the uncatalyzed reaction to very small, and in one case, within experimental error of zero. We propose that in the former instance, where the entropic penalty is large, there is an enzyme conformational change that is concomitant with the organization of the substrate (Scheme 1). In this case, the binding event does not necessarily organize (or fold) the substrate nor does the loop or lid over the active site close. Instead, this occurs in subsequent steps which incur an entropic penalty. In the enzymes for which the entropic contribution to the *ES* to ES^\ddagger transition is small or negligible, the substrate *and* enzyme are pre-organized by the binding event. In other words, the binding event folds the substrate and closes the loop or lid over the active site.

Chorismate mutase reaction

In solution, chorismate goes from a very mobile reactant state (S) to a more ordered transition state (S^\ddagger) for conversion of chorismate to prephenate, and this change has a ΔS^\ddagger value of -12.9 cal/molK²³ (Table 1). When unfolded, the substrate is solvated in a variety of ways, including structured waters surrounding the hydrophobic expanse. These structured waters are lost to bulk solvent upon substrate folding providing a positive change in entropy which is offset wholly or partly by negative changes in entropy arising from the restrictions imposed in folding of the substrate and from solvation of the developing delocalized charge of the transition state which is not present in the ground state. Therefore, the observed negative entropy of activation for the uncatalyzed reaction is a combination of the effects of such changes as substrate folding, release of structured waters, and solvation of developing charges.

For the enzymatic conversion of chorismate to prephenate, the *K. pneumoniae* and *S. aureofaciens* mutases demonstrate a small change for the conversion from the enzyme-substrate complex to the transition state (-1.1 , -1.6 cal/molK, respectively)¹⁴. It has been argued that the observation of little entropic change from ES to ES^\ddagger indicates that the chorismate is pre-arranged in the active site and only becomes slightly more ordered during this step of the reaction cycle¹⁴. The *E. coli* chorismate mutase demonstrates a ΔS^\ddagger value of -3.0 cal/molK¹⁸, which is within error of the *K. pneumoniae* and *S. aureofaciens* mutase values¹⁴. These three enzymes are therefore considered to be classic entropy traps: the enzyme achieves the conformational constriction of the substrate during formation of the ES so that conversion of ES to ES^\ddagger incurs no large entropic penalty^{14,24}. The *B. subtilis* mutase has ΔS^\ddagger value which is more similar to the uncatalyzed reaction than to the other chorismate mutases (-9.1 cal/molK)¹⁷, leading to the suggestion that the active site exerts less conformational control and overcomes this deficit with a more significant change in enthalpy¹⁷. This compensation allows for the similar ΔG^\ddagger values for all four mutases (15.0 – 17.2 kcal/mol). The temperature dependence of k_{cat} for the chorismate mutase activity of PchB (Figure 2), on the other hand, gives a ΔS^\ddagger value of -12.1 cal/molK, which is within experimental error of the ΔS^\ddagger value of the uncatalyzed reaction. By the same argument, this result suggests that there is no conformational control of the substrate in the active site upon formation of the enzyme-substrate complex. This is contrary to structural biology data^{3,7}, which clearly show that the carboxylates of ligands in the active site are oriented by arginines (Figure 1c). Nevertheless, the data here indicate that the differing protein folds (AroQ versus AroH) do not correlate to the differing conformational control of the substrate in the ES complex. Instead, these data corroborate the idea that these active sites are indeed comparable and structural differences do not explain the relative entropic and enthalpic contributions.

Isochorismate-pyruvate lyase reaction

In solution, isochorismate spontaneously undergoes a Claisen rearrangement to form isoprephenate, which undergoes further reaction to form 3-carboxyphenylpyruvate through the loss of a water molecule (Figure 3). Isochorismate also spontaneously forms salicylate and pyruvate in the elimination reaction. Using an NMR assay and measuring the formation of isoprephenate, 3-carboxyphenylpyruvate, salicylate and pyruvate, Hilvert and colleagues have previously experimentally determined the ΔG^\ddagger values for the uncatalyzed reactions at 333.15 K, 24.8 and 26.2 kcal/mol, respectively²². In the experiments presented here, the uncatalyzed elimination reaction was monitored by measuring increasing salicylate fluorescence allowing for the calculation of the concomitant rearrangement reaction (Figure 4), and the thermodynamic parameters were determined as described in the methods (Table 1). The ΔG^\ddagger values reported in Table 1 are calculated for 298.15 K for direct comparison to the previously reported chorismate mutase values. The ΔG^\ddagger values for the uncatalyzed

reaction calculated for 333.15 K are in good agreement with the ΔG^\ddagger values from Hilvert, with the uncatalyzed rearrangement ΔG^\ddagger value of 25.2 kcal/mol and the elimination ΔG^\ddagger value of 26.4 kcal/mol, but the enthalpic and entropic contributions are somewhat unexpected. We had expected enthalpic and entropic contributions for these reactions to be comparable to those previously reported for the mutase reaction (Table 1). However, the entropic penalty for the isochorismate rearrangement contributes considerably less (-5.22 cal/molK) than that for the chorismate rearrangement (-12.9 cal/molK,²³), whereas the entropic contribution of the uncatalyzed isochorismate elimination reaction is the most significant (-15.77 cal/molK). Indeed, the entropic penalty for the isochorismate elimination is most similar to that of the chorismate rearrangement (-12.9 cal/molK). The thermodynamic parameters of the physiological lyase activity of PchB are the most surprising (Figure 4b). This reaction is clearly enthalpically driven, and has a very large entropic penalty (-24.3 cal/molK), which is more than 1.5-fold greater than that of the uncatalyzed reaction (-15.77 cal/molK).

Rate-determining step

Previous work to determine the rate-determining step for the chorismate mutases comes from several different protein forms and from many different kinds of experiments, with the weight of the evidence favoring a chemistry step that is largely or wholly rate-limiting. First, primary heavy atom isotope effects documented for the independent EcCM domain^{25,26} and BsCM²⁵ were consistent with the hypothesis that chemistry is significantly rate-limiting. Second, the effects of viscosogens on steady state parameters indicate that EcCM is insensitive to changes in viscosity and thus chemistry is fully rate-determining, whereas BsCM showed kinetic parameters that were decreased significantly with increasing glycerol and chemistry was calculated to be ~60-70% rate-determining²⁷. The only caveat is that the uncatalyzed reaction showed a 15% secondary tritium kinetic isotope effect at C3 and C9 whereas no comparable effect was detected for the enzyme-catalyzed reaction of the chorismate mutase-prephenate dehydrogenase (the bi-functional enzyme of which one domain is a chorismate mutase with 23% identity and 46% similarity to EcCM)²⁸. If interpreted in isolation, this would suggest that some physical step is rate-determining. It would be intriguing to learn if this is also true of the EcCM domain from the dehydratase enzyme.

The contribution of loop or lid closing to catalysis

Hur and Bruce concluded from molecular dynamics simulations of EcCM initiated at the loop-closed ES conformer that "...the loop structure at residues 42-48 fluctuates more in the [transition state] than in the [enzyme-substrate complex]," which led to the argument that the active site is *less* stable at the transition state and promotes the idea of a "near attack conformation" for catalysis³¹. In other words, it was argued that the substrate and enzyme are preorganized by formation of the ES and formation of the transition state is inconsequential for catalysis. The theoretical calculations of Skolaski and colleagues suggest that Arg90 of BsCM (comparable to the lysine of the active site loop in the AroQ enzymes) has the greatest stabilization effect and is responsible (with Arg7) for the preorganization effects of the substrate^{32,33}. NMR relaxation dynamics of BsCM showed little movement at Arg90, which is found in a β -strand³⁴. However, these data indicate that the C-terminus serves as a lid and there is substantial ordering of flexible residues upon ligand binding³⁴. PchB shows a dramatic change in the active site between the apo- and ligand-bound structures with a disorder-to-order transition of the loop^{3,7}, promoting the hypothesis that active site loop dynamics are important for catalysis. These combined data for both the AroH and AroQ enzymes suggest that loop or lid movement is involved in the catalytic cycle and should be considered in entropic models for catalysis. In agreement with this idea, changes to less negative values of ΔS^\ddagger have been attributed to decreasing phosphate gripper

loop size in orotidine 5'-monophosphate decarboxylases²⁹, suggesting that active site loop mobility contributes to observed entropy changes for conversion of the enzyme-substrate complex to the transition state.

Conclusions

With the predominance of evidence indicating that chemistry is rate-limiting and evidence for a conformational change in the loop or lid closing the active site, we propose the model shown in Scheme 1. Since the reactant state for k_{cat} is the enzyme-substrate complex, a reactive conformation of the substrate may not be formed upon binding of substrate to the enzyme ($E_{\text{open}}S_{\text{unfolded}}$). Instead, the conformer for catalysis ($E_{\text{closed}}S_{\text{folded}}$) is formed along the reaction coordinate approaching the transition state (ES^{\ddagger}), or in line with classical transition state theory, the reactive substrate conformation is formed at the transition state. The ordering of substrate and loop therefore both contribute to the large entropic penalty for the overall ES to ES^{\ddagger} transition. These substrate and loop ordering steps may be sequential as shown in the scheme, or may be concerted: closing of the active site loop may force the substrate into its folded form for catalysis. For the chorismate mutase reactions with no entropic penalty for the ES to ES^{\ddagger} transition, substrate binding may promote closing of the active site (forming $E_{\text{closed}}S_{\text{folded}}$) and therefore the entropy change for this transition is approximately zero.

Acknowledgments

We are grateful to T. C. Gamblin for spectrometer use and R. L. Schowen for insightful discussions. This publication was made possible by funds from the Kansas Masonic Cancer Research Institute, by NIH award number P20 RR016475 from the INBRE Program of the National Center for Research Resources, and by NIH award number R01 AI77725 from the National Institute for Allergy and Infectious Disease.

References

1. DeClue MS, Baldrige KK, Kunzler DE, Kast P, Hilvert D. *J Am Chem Soc.* 2005; 127:15002–15003. [PubMed: 16248620]
2. Gaille C, Kast P, Haas D. *J Biol Chem.* 2002; 277:21768–75. [PubMed: 11937513]
3. Luo Q, Olucha J, Lamb AL. *Biochemistry.* 2009; 48:5239–5245. [PubMed: 19432488]
4. Gallagher DT, Mayhew M, Holden MJ, Howard A, Kim KJ, Vilker VL. *Proteins.* 2001; 44:304–11. [PubMed: 11455603]
5. Nakai T, Mizutani H, Miyahara I, Hirotsu K, Takeda S, Jhee KH, Yoshimura T, Esaki N. *J Biochem.* 2000; 128:29–38. [PubMed: 10876155]
6. Spraggon G, Kim C, Nguyen-Huu X, Yee MC, Yanofsky C, Mills SE. *Proc Natl Acad Sci USA.* 2001; 98:6021–6. [PubMed: 11371633]
7. Zaitseva J, Lu J, Olechowski KL, Lamb AL. *J Biol Chem.* 2006; 281:33441–9. [PubMed: 16914555]
8. Stewart J, Wilson DB, Ganem B. *J Am Chem Soc.* 1990; 112:4582–4584.
9. Lee AY, Karplus PA, Ganem B, Clardy J. *J Am Chem Soc.* 1995; 117:3627–3628.
10. Chook YM, Gray JV, Ke H, Lipscomb WN. *J Mol Biol.* 1994; 240:476–500. [PubMed: 8046752]
11. Chook YM, Ke H, Lipscomb WN. *Proc Natl Acad Sci USA.* 1993; 90:8600–3. [PubMed: 8378335]
12. Ladner JE, Reddy P, Davis A, Tordova M, Howard AJ, Gilliland GL. *Acta Crystallogr.* 2000; D56:673–83.
13. Lee AY, Stewart JD, Clardy J, Ganem B. *Chem Biol.* 1995; 2:195–203. [PubMed: 9383421]
14. Gorisch H. *Biochemistry.* 1978; 17:3700–5. [PubMed: 100134]
15. Camacho C, Coulouris G, Avagyan V, Ma N, Papadopoulos J, Bealer K, Madden TL. *BMC Bioinformatics.* 2009; 10:421. [PubMed: 20003500]
16. Huang X, Miller W. *Adv Appl Math.* 1991; 12:373–381.
17. Kast P, Asif-Ullah M, Hilvert D. *Tetrahedron Lett.* 1996; 37:2691–1694.

18. Galopin CC, Zhang S, Wilson DB, Ganem B. *Tetrahedron Lett.* 1996; 37:8675–8678.
19. Schmidt K, Leistner E. *Biotech & Bioeng.* 1995; 45:285–291.
20. Rieger CE, Turnbull JL. *Prep Biochem Biotechnol.* 1996; 26:67–76. [PubMed: 8744423]
21. Connors, KA. *Chemical Kinetics. The Study of Reaction Rates in Solution.* Wiley-VCH Publishers; New York: 1990.
22. DeClue MS, Baldrige KK, Kast P, Hilvert D. *J Am Chem Soc.* 2006; 128:2043–51. [PubMed: 16464106]
23. Andrews PR, Smith GD, Young IG. *Biochemistry.* 1973; 12:3492–8. [PubMed: 4731190]
24. Westheimer FH. *Adv Enz Rel Areas Mol Biol.* 1962; 24:441–482.
25. Gustin DJ, Mattei P, Kast P, Wiest O, Lee L, Cleland WW, Hilvert D. *J Am Chem Soc.* 1999; 121:1756–1757.
26. Wright SK, DeClue MS, Mandal A, Lee L, Wiest O, Cleland WW, Hilvert D. *J Am Chem Soc.* 2005; 127:12957–64. [PubMed: 16159290]
27. Mattei P, Kast P, Hilvert D. *Eur J Biochem.* 1999; 261:25–32. [PubMed: 10103029]
28. Addadi L, Jaffe EK, Knowles JR. *Biochemistry.* 1983; 22:4494–501. [PubMed: 6354259]
29. Toth K, Amyes TL, Wood BM, Chan KK, Gerlt JA, Richard JP. *Biochemistry.* 2009; 48:8006–13. [PubMed: 19618917]
30. Coquelle N, Fioravanti E, Weik M, Vellieux F, Madern D. *J Mol Biol.* 2007; 374:547–62. [PubMed: 17936781]
31. Hur S, Bruice TC. *Proc Natl Acad Sci USA.* 2002; 99:1176–81. [PubMed: 11818529]
32. Szeftczyk B, Claeysens F, Mulholland AJ, Sokalski WA. *Int J Quant Chem.* 2007; 107:2274–2285.
33. Szeftczyk B, Mulholland AJ, Ranaghan KE, Sokalski WA. *J Am Chem Soc.* 2004; 126:16148–59. [PubMed: 15584751]
34. Eletsky A, Kienhofer A, Hilvert D, Pervushin K. *Biochemistry.* 2005; 44:6788–99. [PubMed: 15865424]

Abbreviations and Full Textual Notes

AroH	chorismate mutase structural family of which BsCM is a member
AroQ	chorismate mutase structural family of which EcCM is a member
BsCM	<i>Bacillus subtilis</i> chorismate mutase
CM	chorismate mutase
EcCM	<i>E. coli</i> chorismate mutase
ES	enzyme-substrate complex
ES[‡]	transition state of enzyme-catalyzed reaction
IPL	isochorismate-pyruvate lyase
KpCM	<i>Klebsiella pneumoniae</i> chorismate mutase
PchB	isochorismate-pyruvate lyase from <i>Pseudomonas aeruginosa</i>
S[‡]	transition state of uncatalyzed reaction
SaCM	<i>Streptomyces aureofaciens</i> chorismate mutase
TSA	transition state analogue

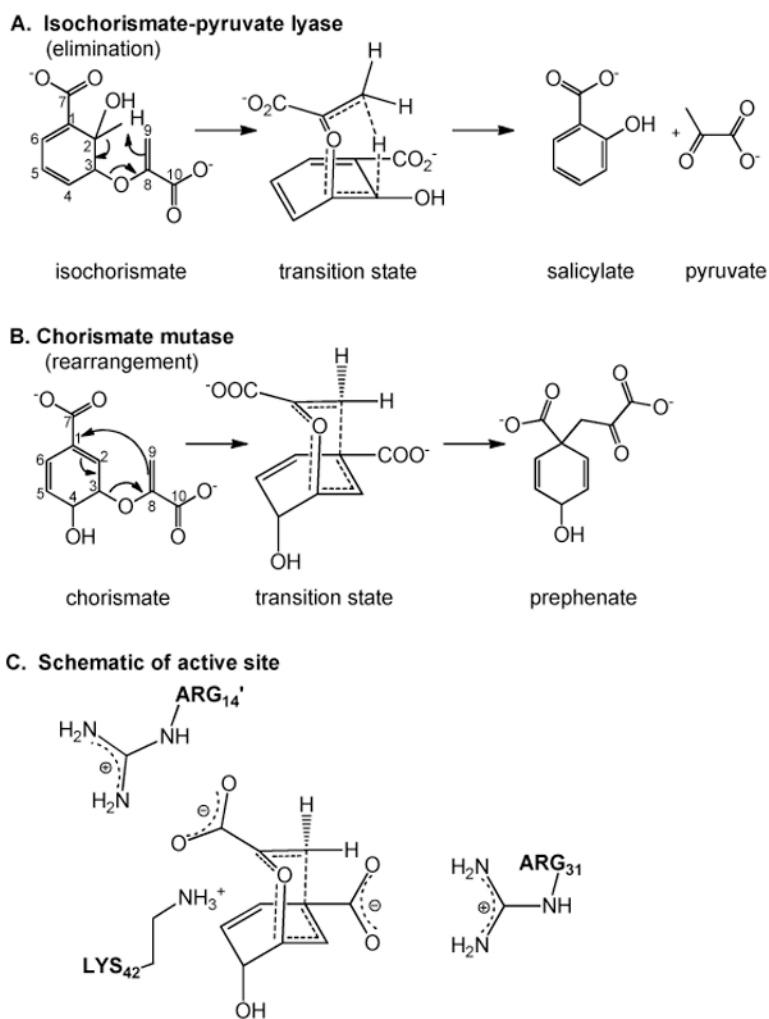


Figure 1.

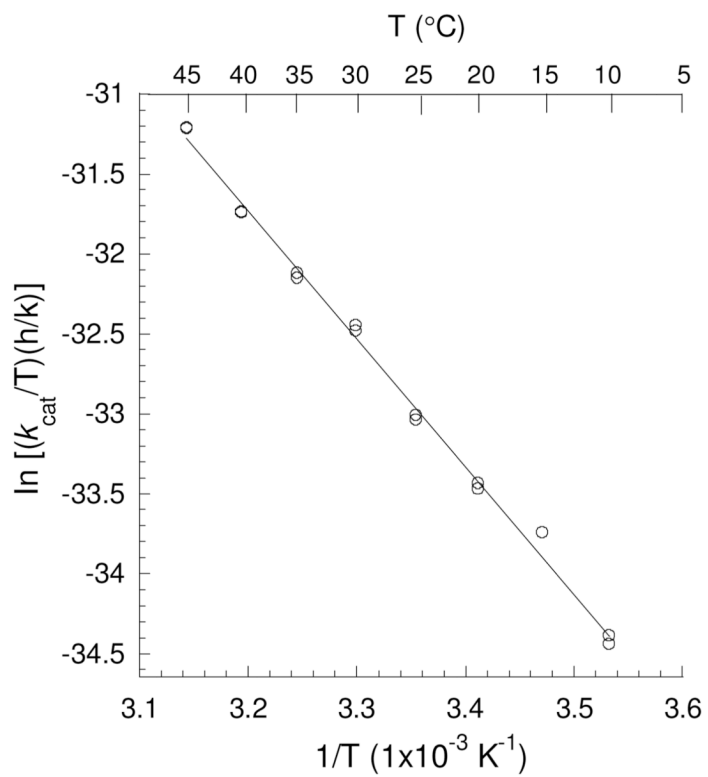


Figure 2. Temperature dependence of k_{cat} for the chorismate mutase reaction of PchB (\circ).

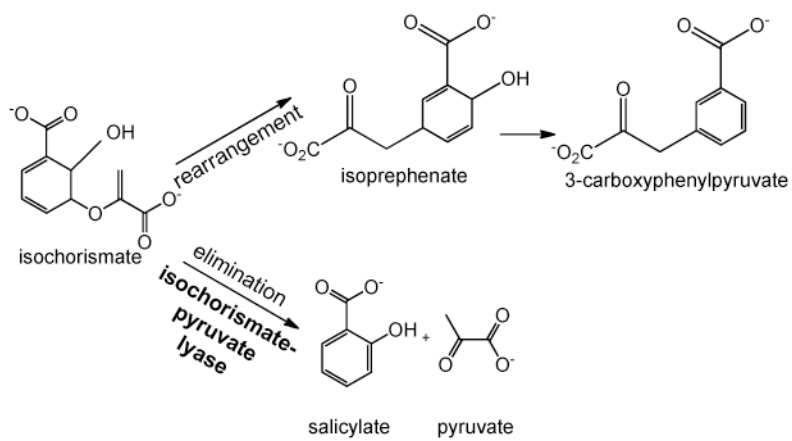


Figure 3. Thermal decomposition of isochorismate. Reaction catalyzed by PchB in bold.

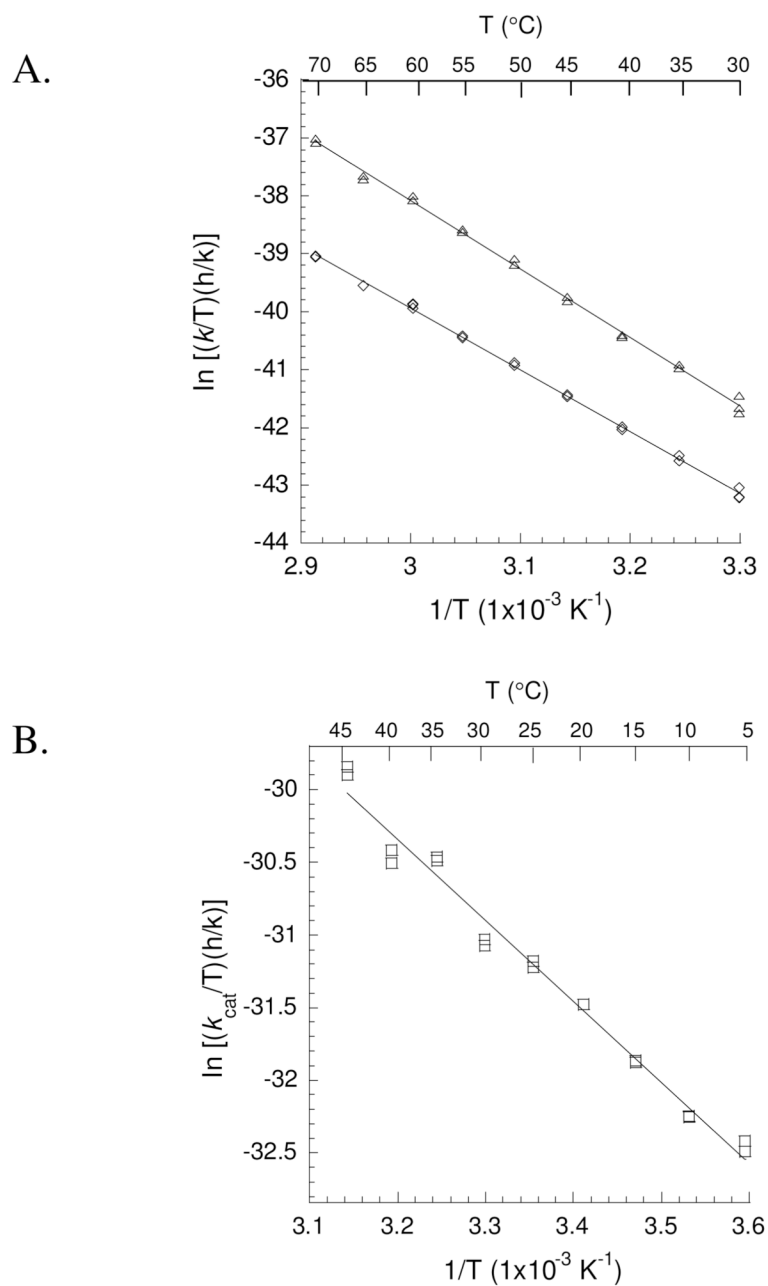


Figure 4. Isochorismate-pyruvate lyase. A) Temperature dependence of the uncatalyzed isochorismate elimination reaction (\diamond) and the uncatalyzed isochorismate rearrangement reaction (Δ). B) Temperature dependence of k_{cat} for the isochorismate-pyruvate lyase reaction of PchB (\square).

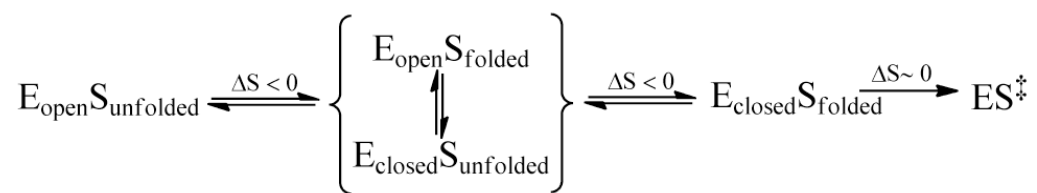
**Scheme 1.**

Table 1

Comparison of the thermodynamic parameters for the mutase and lyase reactions.

Activity	ΔG^{\ddagger} *	ΔH^{\ddagger} *	ΔS^{\ddagger} *	Structural family
	kcal/mol	kcal/mol	cal/mol K	
chorismate \rightarrow prephenate				
Uncatalyzed rearrangement ^a	24.5	20.7 \pm 0.4	-12.9 \pm 0.4	
PchB CM ^b	19.53 \pm 0.01	15.9 \pm 0.2	-12.1 \pm 0.6	AroQ
<i>B. subtilis</i> CM ^c	15.4	12.7 \pm 0.4	-9.1 \pm 1.2	AroH
<i>E. coli</i> CM ^d	17.2	16.3 \pm 0.5	-3.0 \pm 1.6	AroQ
<i>S. aureofaciens</i> CM ^e	15.0	14.5 \pm 0.4	-1.6 \pm 1.1	AroH
<i>K. pneumoniae</i> CM ^e	16.2	15.9 \pm 0.4	-1.1 \pm 1.2	AroQ
chorismate \rightarrow <i>p</i> -hydroxybenzoate + pyruvate				
Uncatalyzed elimination ^a	25.7	23.6 \pm 2.8	-6.9 \pm 1.5	
isochorismate \rightarrow isoprephenate				
Uncatalyzed rearrangement ^f	25.04 \pm 0.03	23.48 \pm 0.06	-5.22 \pm 0.01	
isochorismate \rightarrow salicylate + pyruvate				
Uncatalyzed elimination ^f	25.90 \pm 0.02	21.19 \pm 0.03	-15.77 \pm 0.02	
PchB IPL ^f	18.47 \pm 0.03	11.2 \pm 0.1	-24.3 \pm 0.2	AroQ

* ΔG

† calculated at 298.15K

^a Andrews, Smith and Young (1973). *Biochemistry*, 12, 3492-3498.^b Figure 2^c Kast, Asif-Ullah, Hilvert (1996). *Tetr Lett*, 37, 2691-2694.^d Galopin, Zhang, Wilson, Ganem (1996) *Tetr Lett*, 48, 8675-8678^e Gorisch (1978). *Biochemistry*, 17, 3700-3705.^f Figure 4